

ARPES results on Sr_2RuO_4 : Fermi surface revisited

A. V. Puchkov and Z.-X. Shen

Department of Applied Physics, Stanford University, Stanford, California 94305-4045

T. Kimura

Joint Research Center for Atom Technology, Tsukuba 305-0046, Japan

Y. Tokura

*Joint Research Center for Atom Technology, Tsukuba 305-0046, Japan
and Department of Applied Physics, University of Tokyo, Tokyo 113-0033, Japan*

(Received 17 July 1998)

The electronic band structure of Sr_2RuO_4 has attracted considerable attention recently. However, it has also become a subject of an important controversy. Results of de Haas–van Alphen experiments yielded a Fermi surface consisting of two electronlike and one holelike sheets, in good agreement with the theoretical predictions. At the same time, results of angle-resolved photoemission spectroscopy (ARPES) measurements yielded *one* electronlike and *two* holelike sheets suggesting an extended van Hove singularity (evHS) similar to that found in cuprate high-temperature superconductors. In an effort to resolve this controversy we performed an extensive ARPES study using various incident photon energies. We found no conclusive evidence for an evHS. [S0163-1829(98)50644-3]

Sr_2RuO_4 (Sr214) is a highly two-dimensional metal and a superconductor with $T_c \approx 1$ K.¹ Its layered structure is remarkably similar to that of high-temperature superconductors with RuO_2 planes taking the place of CuO_2 planes. Understanding the electronic structure of Sr214 could provide critical information on the importance of electronic correlations in quasi-two dimensional (2D) materials and their relation to high-temperature superconductivity. Several studies have been performed recently to determine the Fermi surface of Sr214. The results of de Haas–van Alphen (dHvA) experiments yielded a Fermi surface consisting of two electronlike pieces and one holelike piece,² in good agreement with the band-structure calculations.^{3,4} However, based on the results of their angle-resolved photoemission spectroscopy (ARPES) experiments, several research groups reported a Fermi surface consisting of *one* electronlike and *two* holelike pockets with an extended van Hove singularity (evHS) at $(\pi, 0)$ (or M point).^{5,6} Since an evHS was also observed in the cuprate high-temperature superconductors, an important connection has been made between Sr214 and the cuprates.⁵ The main experimental result that led the ARPES groups to a conclusion about the existence of an evHS was an observation of an extremely narrow, very weakly dispersing peak close to the Fermi energy E_F that dominates the ARPES spectra obtained in a Brillouin zone (BZ) area close to M . Since the peak never crosses E_F , it was asserted that there is only one Fermi-level crossing along the Γ - M line as opposed to two predicted by the band-structure calculations and observed experimentally in the dHvA experiments. A “missing” crossing was reported on the M - X line, where two crossings were found, as opposed to one according to the band-structure calculations and the dHvA results. The apparent disagreement between the results of two major experimental techniques has attracted significant attention.⁷

Here we report ARPES results obtained at several incident photon energies $h\nu$. We uncovered a very sharp dependence of the intensity of the peak at M on $h\nu$, suggesting a strong $h\nu$ dependence of the corresponding matrix element. Since such a behavior is not normally expected for an ARPES feature associated with a bulk electronic energy band, we have performed extensive ARPES measurements at $h\nu = 26.4$ eV where the peak is severely suppressed. Our results indicate only *one* Fermi-level crossing along the M - X line and *two* crossings along Γ - X line, in agreement with dHvA results.

For the ARPES experiments samples were cleaved *in situ* in vacuum better than 5×10^{-11} torr. Samples were cleaved and measured at temperature $T = 20$ K. Photons at various energies were generated on the undulator beamline 5-3 at the Stanford Synchrotron Radiation Laboratory (SSRL). The instrumental energy resolution was 35 meV. Several samples were measured and the results were found to be consistent with each other. E_F was determined independently from measurements performed on polycrystalline Au film, electrically connected to a sample. Prior to ARPES measurements, samples were characterized and aligned using Laue diffraction. Sharp, dispersive valence-band peaks as well as an absence of a well known contamination or degradation derived feature at about 10 eV (Ref. 8) speak for a good surface quality.

In Figs. 1(a) and 1(b) we show energy distribution curve (EDC) spectra obtained along the Γ - M line at $h\nu = 22.4$ eV and $h\nu = 26.4$ eV. The Sr214 BZ and the \mathbf{k} -space locations where the spectra were obtained are shown in Fig. 1(d). While the spectra are very similar near Γ , the similarity breaks down near M . Here the spectra obtained at $h\nu = 22.4$ eV are dominated by a resolution-limited almost non-dispersive peak close to E_F , while in the EDC's obtained at $h\nu = 26.4$ eV this feature is absent or severely suppressed.

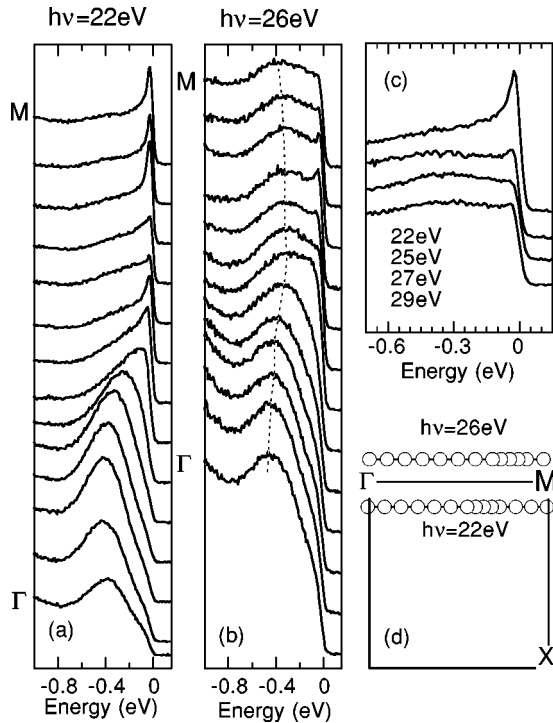


FIG. 1. (a) and (b) show EDC spectra obtained along the Γ - M line at $h\nu = 22.4$ eV and $h\nu = 26.4$ eV. High binding-energy background was subtracted and intensity of the spectra was normalized to an arbitrary value, not the same for (a) and (b). (c) $h\nu$ dependence of the EDC spectra at M point. (d) Experimentally measured BZ points corresponding to the spectra shown in (a) and (b).

The $h\nu$ dependence of the peak at M is shown in Fig. 1(c). We note that the peak disappearance is not a result of radiation damage at higher $h\nu$ since the spectra were taken in order of decreasing $h\nu$. It is usually a good approximation that intensity of an EDC spectrum is $I(\omega, \mathbf{k}) = |M(\omega, \mathbf{k}, \nu)|^2 A(\omega, \mathbf{k}) f_{FD}(\omega)$ where $A(\omega, \mathbf{k})$ is a one-electron spectral function and $f_{FD}(\omega)$ is a Fermi-Dirac function. Therefore, the results suggest strong $h\nu$ dependence for a matrix element $M(\omega, \mathbf{k}, \nu) = |\langle \psi_f | \mathbf{p} \cdot \mathbf{A} | \psi_i \rangle|^2$, where $\psi_{i,f}$ are the initial and final electronic states corresponding to the narrow feature. Such a strong dependence would be quite surprising and unusual for a quasiparticle peak. On the other hand, somewhat similar behavior has been observed before in YBa₂Cu₃O_{6.9} (YBCO), where it was attributed to a surface state.⁹ In addition, the M -point peak is much sharper than the rest of the features seen in Sr214, but is similar to the YBCO surface-state peak. A similar feature was observed in two-plane ruthenium oxide Sr₃Ru₂O₇, although at a different BZ location.¹⁰ In a less directly related case, a surface state of Al also shows strong photon energy dependence.¹¹ Considering that it was the narrow peak that was interpreted as evidence for a van Hove singularity at M in Sr214,^{5,6} the new result on the extremely sharp dependence of its intensity on $h\nu$ makes it necessary to reexamine this conclusion. We also note that the intense peak near M almost completely masks a weakly dispersive peak at about 0.4 eV below E_F . In fact, a flat band below E_F is expected from the results of band-structure calculations, although its energy was predicted to be somewhat higher, ≈ 0.9 eV.^{3,4}

In Figs. 2(a)–(c) we plot EDC spectra obtained along the

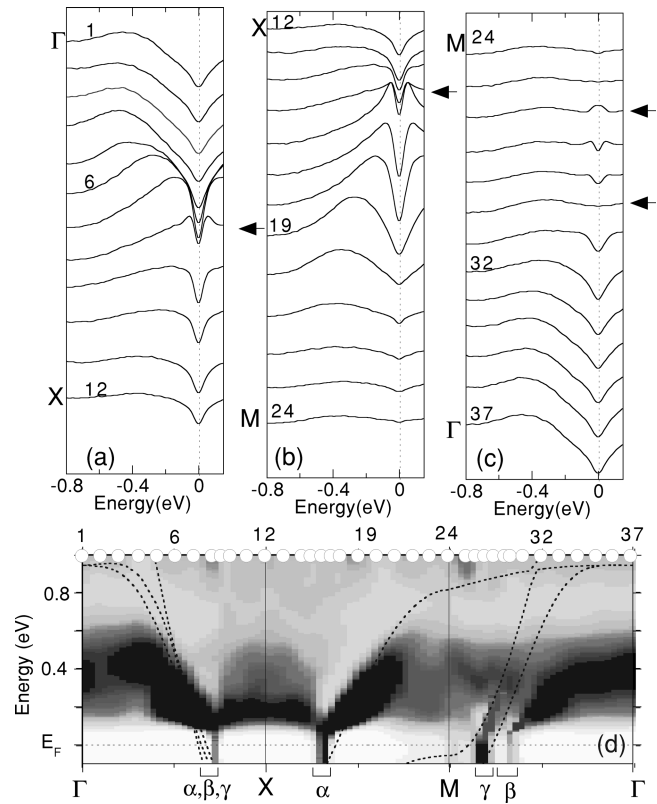


FIG. 2. (a)–(c) EDC spectra obtained at $h\nu = 26.4$ eV along the Γ - X - M - Γ line and symmetrized as discussed in the text. Possible Fermi-level crossings are marked by the arrows. (d) A gray-scale plot of second derivative of the spectra presented in panels (a)–(c). On the top of the panel we show \mathbf{k} locations of the points measured. The dashed lines are the results of the theoretical calculations.

Γ - X - M - Γ line at $h\nu = 26.4$ eV. Prior to plotting, the experimental spectra were symmetrized with respect to E_F , using a procedure suggested by Norman *et al.*¹² The intensity of the symmetrized spectrum $I_s(E)$ is obtained as $I_s(E) = I(E = E_b) + I(E = -E_b)$, where $I(E_b)$ is an intensity of the raw data as a function of binding energy. This removes a Fermi-Dirac edge while at $|E|$ larger than the experimental energy resolution, in our case $|E| \geq 35$ meV, $I_s(E)$ remains the same as the experimentally measured $I(\pm E_b)$. The reason for performing the above procedure is twofold. First, in the next paragraph we will be interested in an energy derivative of the EDC spectra. Removing Fermi-Dirac edge eliminates a corresponding spurious peak in the derivative spectra. Second, spectra symmetrization provides the following convenient way to visually identify Fermi-level crossings. If an EDC spectrum corresponds to a \mathbf{k} location where an electronic band is below E_F , the midpoint of the leading edge of the corresponding ARPES peak is expected to be at the positive binding energies. Therefore, symmetrization will produce a valley in $I_s(E)$ at $E = 0$. If, however, an EDC spectrum corresponds to a Fermi-level crossing, the midpoint is expected to be close to zero binding energies (or even at the negative binding energies due to finite-energy resolution) and symmetrization will produce a plateau (or a peak due to the high binding energy falloff) in $I_s(E)$ at $E = 0$. At \mathbf{k} 's where the band is above E_F the midpoint recedes to positive binding energies so that a valley is expected again. Since in a real

ARPES experiment \mathbf{k} space is probed discretely, to identify Fermi-level crossings one may use spectra with the shallowest valleys instead of the plateaus, which occurs for $\mathbf{k}=\mathbf{k}_F$ only, and thus can be easily missed. Several such \mathbf{k} locations can be identified in the spectra in Figs. 2(a)–2(c) as is indicated by the arrows. It is especially important that two crossings can be seen along the Γ - M line. This is consistent with the results of the dHvA experiments and band structure calculations.

Taking a second derivative of EDC spectra and plotting it as a function of \mathbf{k} and binding energy allows one to trace dispersive ARPES peaks, corresponding to electronic bands, along the high-symmetry lines in a BZ. Such a plot is presented in Fig. 2(d). Before differentiating, the EDC spectra of Figs. 1(a)1(c) were smoothed and interpolated to a regular \mathbf{k} grid at every binding energy to achieve a uniform shading. The gray scale was chosen to emphasize negative values of a second derivative. The experimental plot is dominated by a weakly dispersive band at about 0.4 eV below E_F . It crosses E_F close to X , at locations marked as α , forming a hole pocket. The high intensity between the two crossings near X is due to a receding peak after a band has crossed the Fermi level. The important observation is that *no more crossings are observed* along the X - M line. On the other hand, along the M - Γ line there seem to be *two* bands crossing E_F at \mathbf{k} locations marked γ and β . This is in agreement with the band-structure calculations (dashed lines⁴) and the results of dHvA experiment. Boxes with width representing experimental uncertainty are placed at \mathbf{k} 's where Fermi level crossings were observed in the raw data of Figs. 2(a)–2(c). Both approaches indicate E_F crossings at the same \mathbf{k} locations. We note that while positions of the Fermi-level crossings are in reasonable agreement with the results of band-structure calculations, the bands seem to be much shallower than expected theoretically. From this energy renormalization we estimate the electron effective mass to be $m^*\approx 2.5$, in agreement with the results of dHvA Ref. (2) and infrared optical experiments.¹³

To perform one more test we have chosen the spectral weight (SW) approach to determining a Fermi surface.^{10,14–16} This approach takes advantage of the fact that an electron occupation number $n(\mathbf{k})$ can be written as $n(\mathbf{k})=\int_{-\infty}^{\infty}A(\omega,\mathbf{k})f_{FD}(\omega)d\omega$. In a sudden approximation intensity of an EDC spectrum is $I(\omega,\mathbf{k})=|M(\omega,\mathbf{k})|^2A(\omega,\mathbf{k})f_{FD}(\omega)$. Therefore, if the matrix element does not change very rapidly, ω and \mathbf{k} dependence of EDC spectra mimics closely that of $A(\omega,\mathbf{k})$. If Δ_n is the largest quasiparticle bandwidth then integrating over energy a set of EDC spectra obtained on a sufficiently dense \mathbf{k} grid $\int_{-\Delta_n}^{\Delta_n}I(\omega,\mathbf{k})$, one obtains $n(\mathbf{k})$ modulated by the matrix element. Alternatively, one can choose to integrate over a narrow energy window centered at E_F , $\int_{-\Delta E}^{\Delta E}I(\omega,\mathbf{k})d\omega$, to obtain $n(\mathbf{k},\Delta E)$. Roughly, $n(\mathbf{k},\Delta E)$ is a fraction of the total $n(\mathbf{k})$ that includes only electrons with energies ΔE away from the Fermi energy. It is nonzero only for \mathbf{k} 's where an electronic band $E(\mathbf{k})$ is close enough to the Fermi energy, $E_F-E(\mathbf{k})\leq\Delta E$.

While the SW approach is generally quite appealing, there are a number of complications. While a comprehensive review can be found elsewhere,^{14,16} we mention a few of the

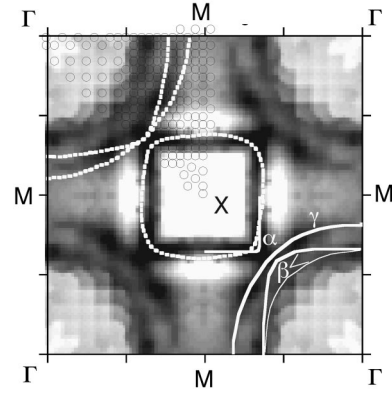


FIG. 3. A 2D distribution of $N(\mathbf{k})=\int_{-50\text{meV}}^{50\text{meV}}I(\omega,\mathbf{k})d\omega$, where $I(\omega,\mathbf{k})$ is an EDC intensity obtained using $h\nu=26.4$ eV. Locations of the measured points are shown in the upper left corner. Darker regions indicate higher intensity. The Fermi surface deduced from the spectral weight plot is shown in the lower right corner (solid lines). Theoretically obtained Fermi surface is plotted by the broken lines. There are two electronlike pieces (β and γ) and one holelike (α). Piece β is not clearly resolved along the Γ - X line and can be drawn as both the narrow and the bold solid lines. However, since we do not observe a separate crossing for β in Fig. 2(d), the bold line is a better representation.

most serious potential problems. First, there are no intrinsic reasons to believe that the matrix element does not change significantly on the scale of a BZ. This may lead to significantly different contributions from bands having different orbital character. A gradient method was suggested to solve this problem.^{14,16} However, since taking derivative greatly amplifies experimental noise, a very fine mesh in \mathbf{k} space is usually required. We could not achieve the necessary precision in our experiment. We also found that while both the broad energy window and the narrow energy window integration techniques produced similar results, using the latter allowed us to achieve a better contrast. However, this technique does not provide a mechanism to distinguish between a band that actually crosses the Fermi level and a flat band that enters the window of integration but never crosses E_F , prompting a certain degree of caution. Fortunately, one can compare the $n(\mathbf{k})$ map with the experimentally obtained dispersions, such as that shown in Fig. 2(d), to check for a possibility of a flat band.

EDC spectra were measured at 200 points \mathbf{k}_i in 1/8 of the BZ, as is shown in the upper right quadrant of Fig. 3. The rest of the BZ was assumed to be tetragonally symmetrical. Incident photon energy $h\nu=26.4$ eV was used. The resulting spectra were integrated over the binding-energy window from 0.05 to -0.05 eV giving a set $N(\mathbf{k}_i)=n(\mathbf{k}_i,\Delta E=0.05$ eV) that was interpolated to a regular grid in \mathbf{k} space using a simple formula $N(\mathbf{k})=\sum_i N(\mathbf{k}_i)\exp[-(|\mathbf{k}-\mathbf{k}_i|/\Delta k)^2]/\sum_i \exp[-(|\mathbf{k}-\mathbf{k}_i|/\Delta k)^2]$, where \mathbf{k} is a wave number on a regular grid and Δk is representative of an experimental angular resolution. The resulting 2D plot is presented in Fig. 3 with darker regions corresponding to a larger SW.

The Fermi surface deduced from the SW plot is shown by the solid lines in the lower right corner of Fig. 3. The Fermi surface predicted by the band-structure calculations is shown with the broken lines.⁴ The shape and size of the holelike

pocket centered at X (piece α) and the larger of the electron pockets (γ) are in excellent agreement with the theoretical predictions. The smallest of the electron pockets (β) is clearly resolved along the edge of the BZ (Γ - M) but not along the diagonal direction Γ - X . As a result, it can be drawn both as the narrow solid line and as the bold solid line. However, since no separate E_F crossing was observed for β along Γ - X in Fig. 2(d), we believe that the bold line is a better representation. The increased SW at the position of the narrow line is probably due to both γ and β entering the window of integration. The total Fermi-surface volume is 3.85 compared to 4 expected theoretically. Considering that the experimental angular resolution was $\pm 1^\circ$, which translates into appropriately $\pm 2.5\%$ of the Brillouin vector, we find an agreement between the Fermi surface predicted theoretically and that obtained in our ARPES experiment to be quite satisfactory.

The net experimental result of this and previous ARPES studies, prior to any interpretation, is as follows. (i) An intense peak, with resolution-limited width and almost no visible dispersion, is observed near M if an incident photon energy $h\nu \leq 23$ eV is used. This peak provided key evidence for an evHS suggested previously, *inconsistent* with the results of either the dHvA experiment or band structure calculations. (ii) The peak is severely suppressed or disappears at higher $h\nu$. An ARPES study performed at $h\nu = 26.4$ eV produced a Fermi surface *consistent* with the one obtained in the dHvA experiment and band-structure calculations. The above suggests that the ARPES evidence for an evHS is not entirely conclusive. In particular, it is not clear if the narrow peak at M represents a bulk electronic energy band.

While there is not enough direct experimental ARPES information to pinpoint the origin of the narrow peak, we

argue that the overall body of evidence suggests that it does not represent a bulk electronic band. (i) Comparison of ARPES results with the results of dHvA experiments and band-structure calculations clearly supports the above hypothesis. (ii) The characteristic properties of the peak, namely its extreme narrowness, sharp photon energy dependence, and lack of appreciable dispersion, are very unusual for an ARPES feature that has its origin in a bulk band structure. This is corroborated by the fact that as the photon energy is changed the peak intensity becomes severely depressed while EDC spectra at the higher binding energies barely change, hinting that the peak does not disperse towards E_F from the higher binding energies.

In summary, we performed an extensive ARPES study of Sr214. We found that our results provide no conclusive support for an evHS at $(\pi, 0)$, suggested previously. In particular, it is not clear if the narrow ARPES peak, which was interpreted as evidence for an evHS, actually results from a bulk electronic band. While more work is required to understand the exact nature of the peak, we note that it is empirically similar to a surface state observed in YBCO.⁹ Among other results we emphasize the possibility of strong electron correlations in Sr214 as is evident from the high values of electronic effective mass $m^* = 2.5$.

We would like to acknowledge useful discussions with E.W. Plummer. SSRL is operated by the DOE Office of Basic Energy Science, Division of Chemical Sciences. The office's Division of Material Science provided support for this research. The Stanford work was also supported by NSF Grant Nos. DMR-9311566 and DMR-9705210. The work at JRCAT was supported in part by the New Energy and Technology Development Organization (NEDO).

¹Y. Maeno *et al.*, Nature (London) (London) **372**, 532 (1994).

²A.P. Mackenzie *et al.*, Phys. Rev. Lett. **76**, 3786 (1996).

³T. Oguchi, Phys. Rev. B **51**, 1385 (1995).

⁴D.J. Singh, Phys. Rev. B **52**, 1358 (1995).

⁵T. Yokoya *et al.*, Phys. Rev. B **54**, 13 311 (1996).

⁶D.H. Lu *et al.*, Phys. Rev. Lett. **76**, 4845 (1996).

⁷T. Yokoya *et al.*, Phys. Rev. Lett. **78**, 2272 (1997); A.P. Mackenzie *et al.*, *ibid.* **78**, 2271 (1997).

⁸A. Gulino *et al.*, Phys. Rev. B **51**, 6827 (1995).

⁹M.C. Schabel *et al.*, Phys. Rev. B **57**, 6090 (1998).

¹⁰A.V. Puchkov *et al.*, Phys. Rev. B (to be published).

¹¹H.J. Levinson *et al.*, Phys. Rev. B **27**, 727 (1983).

¹²M.R. Norman *et al.*, cond-mat/9710163 (unpublished).

¹³T. Katsufuji *et al.*, Phys. Rev. Lett. **76**, 26 (1996).

¹⁴M.C. Schabel *et al.*, Phys. Rev. B **57**, 6107 (1998).

¹⁵A. Santoni *et al.*, Appl. Phys. A: Solids Surf. **52**, 299 (1991); P. Aebi *et al.*, Phys. Rev. Lett. **72**, 2757 (1994); M. Randeria *et al.*, *ibid.* **74**, 4951 (1995).

¹⁶Th. Straub *et al.*, Phys. Rev. B **55**, 13 473 (1997).